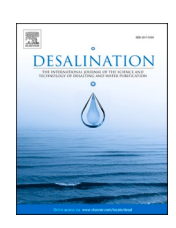
ELSEVIER

Contents lists available at ScienceDirect

Desalination

journal homepage: www.elsevier.com/locate/desal





Coupling of electromembrane processes with reverse osmosis for seawater desalination: Pilot plant demonstration and testing

Luigi Gurreri ^{a,*}, Mariagiorgia La Cerva ^a, Jordi Moreno ^b, Berry Goossens ^c, Andrea Trunz ^{d,*}, Alessandro Tamburini ^a

- a Department of Engineering, University of Palermo, Viale delle Scienze ed. 6, 90128 Palermo, Italy
- ^b REDstack B.V., Graaf Adolfstraat 35G, 8606 BT Sneek, the Netherlands
- ^c FUJIFILM Manufacturing Europe B.V., Oudenstaart 1, 5000 LJ Tilburg, the Netherlands
- ^d Trunz Water Systems AG, Technologie Center, Ahornstrasse 1, CH-9323 Steinach, Switzerland

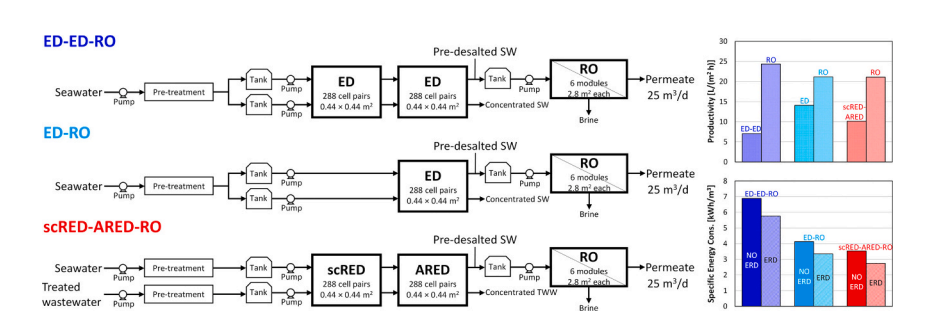
HIGHLIGHTS

- A pilot plant with capacity of 25 m³/ d was developed for seawater desalination.
- ED-ED-RO, ED-RO, and scRED-ARED-RO process schemes were tested.
- Real seawater and secondary wastewater were used, producing drinking water.
- Mean productivity of 10 and 23 L/(m²
 h) in the electromembrane processes and in RO.
- Energy consumption comparable to that of a standalone SWRO system.

ARTICLE INFO

Keywords: Ion-exchange membrane Field test Potable water Hybrid membrane process Impaired water

GRAPHICAL ABSTRACT



ABSTRACT

Reverse osmosis (RO) is the most widespread technology to produce drinking water from seawater (SW). However, the integration of different membrane processes offers interesting alternatives. In this work, electromembrane processes were integrated with RO to desalinate real seawater in a pilot plant with 25 m³/day capacity. Electrodialysis (ED, either two-stage or single stage), shortcut reverse electrodialysis (scRED) and assisted reverse electrodialysis (ARED) pre-desalinated seawater before RO with the ED-ED-RO, ED-RO, and scRED-ARED-RO process schemes. Treated wastewater was used as salt sink in the scRED-ARED tests. The performance of the pilot plant can be summarized as follows: water recovery of \sim 27–51%, productivity of \sim 7–14 L/ (m² h) in the electromembrane processes and of \sim 19–31 L/(m² h) in the RO process, energy consumption of 3.5–8.4 kWh/m³. The ED-RO configuration yielded the maximum productivity of the electromembrane step, while the scRED-ARED-RO integration reached the minimum energy consumption. Overall, the energy performance of the pilot plant (especially in the ED-RO and scRED-ARED-RO schemes) was comparable to that of a standalone SWRO system. The field tests demonstrated that the coupling of electromembrane processes with RO

Abbreviations: AEM, anion-exchange membrane; ARED, assisted reverse electrodialysis; CEM, cation-exchange membrane; ED, electrodialysis; EM, electromembrane; ERD, energy recovery device; ERS, electrode rinse solution; IEM, ion-exchange membrane; MF, Microfiltration; RED, reverse electrodialysis; RO, reverse osmosis; scRED, short-circuit reverse electrodialysis; SW, seawater; SWED, seawater electrodialysis; SWRO, seawater reverse osmosis; SEC, specific energy consumption; TDS, total dissolved solids; TWW, treated wastewater; UF, ultrafiltration.

E-mail addresses: luigi.gurreri@unipa.it (L. Gurreri), a.trunz@trunz.ch (A. Trunz).

^{*} Corresponding authors.

is feasible and suggest the possibility to develop alternative and competitive industrial pants for seawater desalination.

1. Introduction

The increasing global water demand requires challenging solutions for a satisfactory water supply. Due to the abundance of saltwater, desalination will play a crucial role. Today the worldwide capacity of desalination plants is ~100 million m³/day of freshwater, ~60% of which is obtained by using seawater (SW), and ~70% via the reverse osmosis (RO) technology [1,2]. Typical water fluxes of RO modules, which affect the capital cost, are in the range $10-40 \text{ L/(m}^2 \text{ h)}$ [3]. The operating costs are basically due to the energy consumed to pressurize the feedwater. The theoretical minimum energy (thermodynamic limit) consumed to produce freshwater from seawater with 50% water recovery is $\sim 1 \text{ kWh/m}^3$ [4,5]. However, the overpressure required by RO to generate reasonable water fluxes and the steps of intake, pre- and post-treatment, and brine disposal significantly increase the energy consumption. On the other hand, part of the pressure energy can be recovered by pressure exchangers. The specific energy consumption (SEC) of SWRO desalination plants has been reduced significantly in the last decades [4,5], being now in the range 2.5–7 kWh/m³ [5–10].

Electrodialysis (ED) [11] is an emerging technology [12] that holds $\sim 2-3\%$ of the global desalination capacity [1,2,6]. ED desalination plants use brackish water to produce potable water, as ED can compete with RO for low-salinity feeds. Predictions of a process model showed that ED outperforms RO in terms of energy consumption to desalinate feedwater at a concentration lower than 3 g/L [13]. On the other hand, the high cost of the IEMs (in the order of $10-100 \text{ } \epsilon/\text{m}^2$ [14,15], against $\sim 10 \text{ } \epsilon/\text{m}^2$ of the osmotic membrane for RO [16]) still limits a widespread use of ED. However, another study found that ED is economically convenient compared to RO for a feedwater salinity below $\sim 8 \text{ g/L}$ [17].

ED is also versatile for various applications [18,19]. However, it is techno-economically uncompetitive with SWRO yet to produce freshwater by desalinating concentrated solutions like seawater [20–27]. The low concentration of the dilute product (e.g., ~0.5 g/L) and the large concentration gradient between the two compartments (up to \sim 60 g/L) cause low migrative fluxes and high back diffusive fluxes, respectively, in a portion of the stack ending with the outlet, resulting in low net fluxes. This implies that the SWED process has difficulties in reaching the concentration target for drinking water. Multi-staging is an effective strategy to produce potable water by the application of current densities approaching the limiting one of each stage. Moreover, increasing the membrane area reduces the SEC [12]. A process model simulated a twostage SWED process with cross-flow stacks equipped with profiled membranes, predicting low (or high) values of SEC along with low (or high) values of productivity in the range of $\sim 2.3-5.7$ kWh/m³ and \sim 2.6–11.2 L/(m² h), respectively [23]. A three-stage ED system used in experiments with natural seawater (~27 g/L) produced a diluate at 1.9 g/L with an SEC of \sim 3 kWh/m³ and a productivity, here estimated by neglecting water transport, of \sim 6 L/(m² h) [24]. These examples show that multi-stage SWED processes can produce potable water, but only one of the two performance metrics (SEC or productivity) at a time has values comparable with those typical of RO.

The opposite process of ED is reverse electrodialysis (RED), which converts the mixing energy of two solutions at different salt concentration into electrical energy. The RED process has been widely studied in the last decade [15,28–31] and pilot installations have brought the technology maturity to the prototype level [32–36]. However, industrial applications do not exist yet due to the low power density (in the order of 1 W/m^2 for seawater-river water, one order of magnitude more in the case of acidic and alkaline solutions in stacks with bipolar membranes [37]) and high membrane cost.

RED can be a method of simultaneous seawater pre-desalination and

energy recovery by using a salt sink, such as impaired water [38]. An RED stack operated with null external resistance works under short-circuit conditions (scRED), producing the maximum current along with zero voltage, i.e., without energy recovery nor consumption (apart from the pumping energy). Therefore, it yields the maximum desalination degree with a spontaneous process. RED can also be conducted under "assisted" conditions. Assisted reverse electrodialysis (ARED) has hybrid features between ED and RED, as it uses electricity from a power supply (like ED) in addition to that generated by a salinity gradient (like RED) to drive electromigration from the high-salinity compartment to the low-salinity compartment (like RED). By applying a voltage drop of opposite sign compared to RED, the electric current of ARED is higher than the short-circuit value. Therefore, ARED consumes energy by desalting the high-salinity solution either more than RED or with less membrane area than RED.

Hybridization of membrane technologies has been proposed as a strategy for the development of energy efficient desalination processes [10,12,39]. Coupling RO with the abovementioned electromembrane (EM) processes (ED, RED or ARED) offers several solutions. Many studies have focused on minimum liquid discharge concepts where the RO reject brine valorisation is performed via (i) ED and crystallization to recover water and salt, or (ii) ED with bipolar membranes to produce acid and base, or (iii) RED to recover energy [12,19,40].

Other hybrid schemes can be devised with EM processes used as a pre-treatment step before RO to desalinate seawater. The SWED-RO system (Fig. 1a) may enhance the energy efficiency compared to the standalone processes. The partial desalination in the ED stage, which works under milder conditions (i.e., with higher limiting current density, lower back-diffusion and higher current efficiency) than those of the SWED process producing potable water, may be cost-effective [41,42] by achieving high productivity and efficiency [41]. Moreover, the ED versatility in terms of desalination degree and water recovery makes it potentially suitable as pre-treatment before RO. This would then receive a brackish water with lower osmotic pressure that would require lower operating pressures or lower membrane area, and could

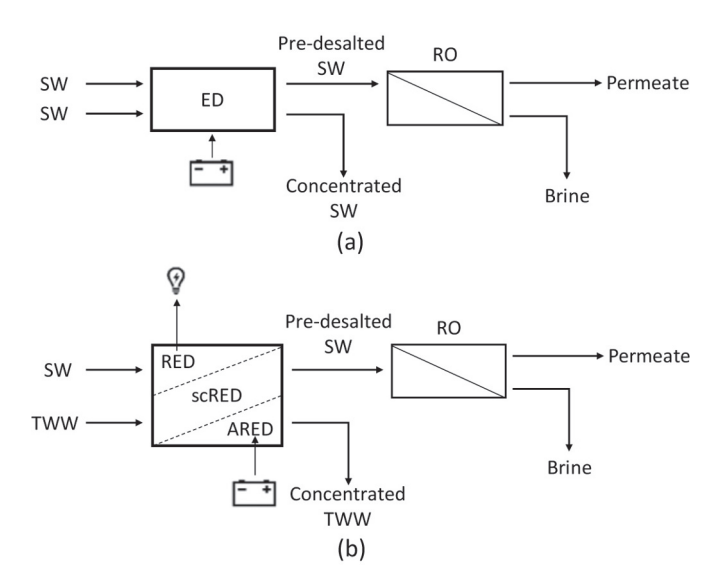


Fig. 1. Schematics of hybrid systems for seawater (SW) desalination with reverse osmosis (RO) coupled with electromembrane pre-treatments: (a) electrodialysis (ED); (b) reverse electrodialysis (RED), short-circuit reverse electrodialysis (scRED) or assisted reverse electrodialysis (ARED) using treated wastewater (TWW) as "salt sink". Adapted from [38].

achieve high water recoveries. By performing batch ED experiments with artificial seawater, Galama et al. [43] used literature data on BWRO and estimated an SEC of the SWED-RO desalination of $\sim 3 \text{ kWh/m}^3$, against an SEC of the standalone SWED higher by 6%. Post et al. [44] performed a cost analysis of desalination processes. In a perspective scenario with high-performance and low-cost IEMs (perfect permselectivity, no water transport, 5 €/m²), the SWED-RO configuration with 80% pre-desalination was effective in reducing the water cost. The authors of the present paper from the University of Palermo presented a cost analysis based on the predictions of process models [38]. Some conditions simulated for the hybrid SWED-RO process (lower voltage and higher number of cell pairs) exhibited a reduction of SEC compared to the standalone SWRO, but it was small. The SWED-RO desalination cost was higher in all cases, showing that the conditions simulated were not optimal. An optimization study of hybrid systems (ED-RO, NF-RO, NF-ED-RO, and FO-ED-RO) for seawater desalination was performed together with a carbon footprint evaluation and a cost analysis [45]. The objective function of minimum SEC was used, and the ED-RO system achieved the lowest value (1.3 kWh/m³) along with a reduction of CO₂ emissions. However, searching for the minimum SEC resulted in low water recoveries (< 30%) and large IEMs area, increasing the water cost.

The ED-RO hybridization was also studied for other applications, including brackish water desalination [46,47], groundwater treatment [48], and near-zero liquid discharge approaches to treat basal aquifer water [49] or desulfurization wastewater [50], showing promising results.

In the RED-RO and ARED-RO couplings for seawater desalination, the EM process is performed by exploiting a sink of salt represented by impaired water that cannot be used directly to produce freshwater, e.g., treated wastewater (Fig. 1b). The energy efficiency of the desalination process is enhanced compared to the ED-RO system thanks to a completely (RED or scRED) or partially (ARED) spontaneous predesalination. The RED process also supplies electrical energy to an external load. RED experiments showed that the salt concentrations in the low-salinity solution that maximize the power density (0.39 W/m^2) were between 0.01 and 0.02 M [51]. This range, which was confirmed by several studies [52,53], corresponds to typical concentrations of treated wastewater (TWW) from biological processes. With real pretreated solutions, a maximum gross power density of 1.43 W/m² was obtained [54]. Therefore, RED using the SW-TWW solutions could be adopted as RO pre-treatment to reduce the SEC. The other option is SWRO-RED, in which RED uses the RO brine-TWW solutions, thus increasing the energy production [51]. However, Li et al. [55] showed a lower SEC for the RED-RO configuration (~0.5 kWh/m³) compared to the RO-RED scheme (~1 kWh/m³). With lab-scale experiments, Vanoppen et al. [56,57] found that, compared to RED, ARED boosts the desalination degree with low energy consumption due to a significant reduction of stack resistance (higher average concentration of the lowsalinity stream) at high current densities. The reduction of resistance and its effects may vanish in large-scale stacks. However, the ARED option can improve the process economics. At high water recoveries (> 40%) the estimated SEC of the ARED-RO process was lower than that of the standalone RO, but larger than that of RED-RO [56]. Nevertheless, the lower membrane requirement of ARED pre-treatments and their resulting lower investment costs reduced the water cost of ARED-RO hybrid systems compared to RED-RO. A water cost reduction compared to the standalone SWRO was found when the IEMs cost was lower than 10 €/m² [56]. Our simulations and economic analysis showed that both RED-RO and ARED-RO may achieve cost savings compared to the standalone SWRO even with a cost for the EM stack of 40 €/m² [38].

The present literature review shows that hybrid schemes coupling EM processes with RO (i.e., ED-RO, RED-RO, and ARED-RO systems) offer new opportunities to reduce the energy consumption and even the specific cost of desalination. However, a poor effort has been devoted to the development of these systems for seawater desalination, and more

studies are needed at pilot-scale to enhance the technological readiness level of emerging processes [12,40]. In this work, we present the first experimental proof-of-concept of electromembrane processes-RO coupling for seawater desalination by the development, construction, and testing of a pilot plant with a capacity of $25~{\rm m}^3/{\rm day}$ working in a real environment. The plant was tested under various operating conditions during a period of about one year, and the collected data are presented and discussed in this paper.

2. Experimental

The pilot installation targeted an integrated ED/RED-RO system with a capacity of $25~{\rm m}^3$ /day of desalinated water. The system was designed to facilitate flexible testing of one stage or two-stage ED/RED/ARED predesalination using real seawater and, in the case of RED or ARED, treated wastewater.

The test location was at the facilities of the municipal wastewater treatment plant located in Burriana (province of Valencia), Spain, which is placed close to the sea. The plant belongs to FACSA, a Spanish private company specialized in water cycle management. The desalination pilot plant was constructed by Trunz in a containerised system (Fig. 2). The programming of the PLC was done in order to perform controlled long-time testing, including a remote monitoring. During the experiments, all parameters (including flow rate, pH, conductivity, electric current, voltage drop and pressure) were measured by the installed instruments and saved by a data acquisition system for later elaboration.

The technical concept of the pilot plant consisted out of three main systems:

- The pre-treatment system of seawater and wastewater, preventing fouling and scaling problems in the membranes of the EM and RO systems;
- 2. The EM system consisting of 2 stacks, which partially desalinated the seawater;
- The RO system, finalising the desalination process to produce drinking water.

2.1. Pre-treatment system

The main physico-chemical characteristics of the two feeds (i.e., seawater and secondary treated wastewater) are reported in Table 1 and Table 2, respectively.

The pre-treatment system was designed to guarantee an advanced protection of the EM-RO units and of the pumps. The goal of the pre-treatment of the feedwater (seawater or wastewater) was to prevent fouling and clogging in the integrated desalination pilot plant by removing suspended solids, organic matter, and microorganisms.

The pre-treatment system had one line dedicated to only seawater and two lines in parallel for wastewater.

As a first pre-treatment step, a sand filtration was used. The advantage of a sand filter is its back-flushing possibility. A cartridge filter (100 μm MF), which is cheap and easily handling, was then chosen as the second step.

The heart of the pre-treatment was an ultrafiltration (UF) module (Inge VK-0069 Dizzer XL 1.5 MB 40 W, Lenntech) that removes organic contamination down to a size of 0.02 μm . The UF pre-treatment was controlled with a manual back and forward flushing and required very little maintenance, ensuring safe operation of the entire system.

In addition, the two lines for wastewater included active carbon filters (Big Blue, $20^{\prime\prime}$ cartridge filter, Pentair) as a further step after ultrafiltration.

2.2. Electromembrane system

Preliminary estimates resulted in the idea to use a 2-stage EM system



Fig. 2. Picture of the integrated EM process-RO pilot plant (left) installed in a container (right) at the FACSA WWTP in Burriana, Spain.

Table 1Physico-chemical properties of seawater samples.

Parameter	Units	Value
Sodium	(mg/L)	12,122.5
Magnesium	(mg/L)	1383.5
Calcium	(mg/L)	619.3
Potassium	(mg/L)	441.3
Chloride	(mg/L)	21,010.2
Sulfate	(mg/L)	2936.0
Bromide	(mg/L)	58.8
Fluoride	(mg/L)	0.8
TOC	(mg/L)	3.6
TC	(mg/L)	30.2
TDS	(mg/L)	38,572.4
Conductivity	(mS/cm)	52.1
pH		7.7
Alkalinity (as CaCO3)	(mg/L)	126.3

Table 2 Physico-chemical properties of secondary treated wastewater samples.

Parameter	Units	Value
TOC	(mg/L)	9
TDS	(mg/L)	1484
Conductivity	(mS/cm)	2.2
pH		7.9
Alkalinity (as CaCO3)	(mg/L)	150
Turbidity	(NTU)	4
Suspended solids (glass fiber)	(mg/L)	5
BOD5	(mg/L)	8
COD	(mg/L)	19

at low flow velocity to perform the pre-desalination of seawater before RO. This system should be characterized by low values of energy consumption. A 1-stage ED system, which requires less membrane area, was also considered, as it is intrinsically characterized by higher values of productivity.

The stacks (REDstack B.V., the Netherlands, Fig. 3) were with cross-flow layout of the fluid streams and each of them contained 288 cell pairs of Fujifilm Type 10 membranes (FUJIFILM Manufacturing Europe B.V., the Netherlands) with active area of 0.44×0.44 m 2 . The main

properties of the membranes are reported in Table 3. Polymeric spacers with woven net and of 260 μm thickness (Deukum GmbH, Germany) were used to separate the membranes and create the channels.

Pt-coated Ti-mesh electrodes (Magneto Special Anodes B.V., The Netherlands) were used. The electrode rinse solution (ERS) was an aqueous solution with 0.5 M Na_2SO_4 . Either FUJIFILM Type 10 or Fumasep® F-10100 (Fumatech GmbH, Germany) CEMs were used as end-membranes confining the electrode compartments (for more details, see the Appendix).

The electrode compartments of the ED stacks were connected to a DC power supply (SM 500-CP-90, Delta Elektronika, The Netherlands). The solutions were fed into the stacks by centrifugal pumps (MDR 85 P3—1V, Johnson Pump).

The pilot installation was used either for Electrodialysis (ED) of seawater or Assisted Reverse Electrodialysis (ARED) of the couple seawater / wastewater. The feed water from the pre-treatment was transferred to either the diluate or the concentrate tank. From these tanks the feed water was then pumped into the ED stacks.

Problems of biofouling and calcium-carbonate scaling in the stacks may be expected. The pre-treatment step based on ultrafiltration was combined with acid dosing in the ED stacks. In addition, the electrodialysis reversal operation (switch every 30 min) was performed. A possibility to perform chemical cleaning-in-place (CIP) was also included.

The combined action of the advanced pre-treatment system, of the polarity reversal, and of the chemical dosage succeeded in the purpose of protecting the pilot plant, allowing a long operation without a performance drop. For industrial applications, concerns may arise on the economic viability of the applied methods. Therefore, purposely devoted studies should address this specific aspect.

The pilot installation was equipped with the necessary tools to measure flow, pressure, temperature, conductivity, and pH in all streams.

2.3. RO system

The RO setup was designed for processing pre-desalinated water from the ED system. The technical considerations for this design were a maximum value of TDS in the feed of ~ 20 g/L, Silt Density Index (SDI) < 2.5 (ensured by the pre-treatment train), permeate flowrate of about

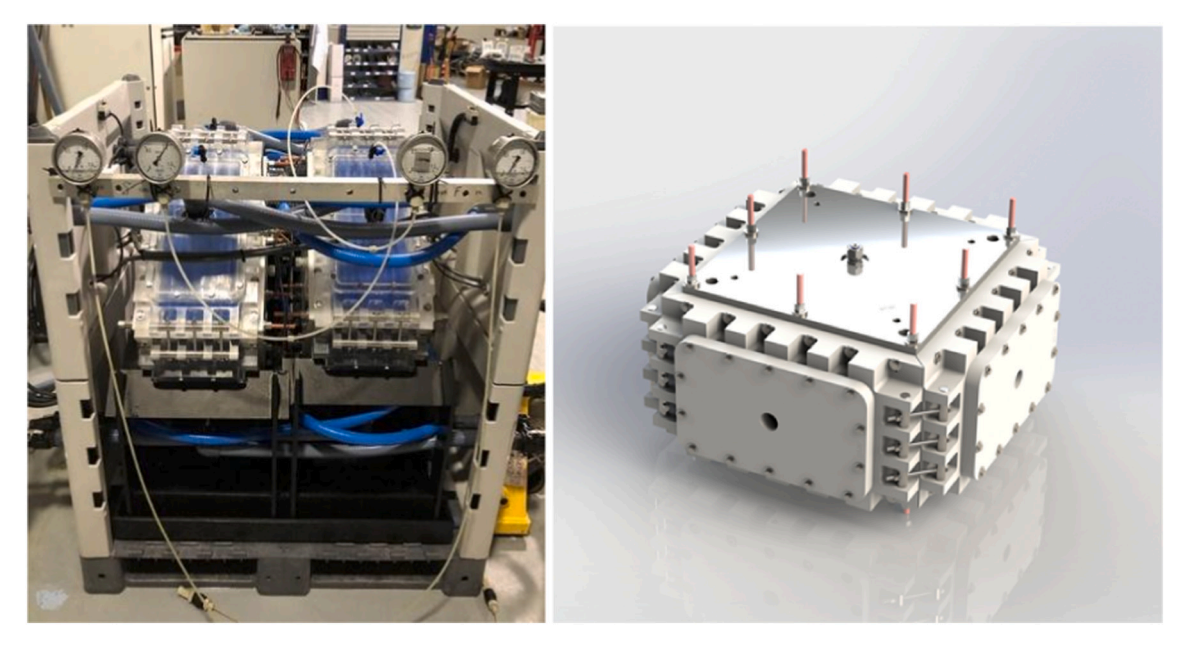


Fig. 3. Picture of the 2-stack EM pilot (left) and 3D drawing of one stack designed by REDstack.

Table 3Properties of the Fujifilm Type 10 ion-exchange membranes used in this study.

	Thickness (dry) [μm]	Areal resistance ^a $[\Omega \text{ cm}^2]$	Permselectivity ^b [%]	IEC [meq/g]	Water permeability [mL/(m² h bar]	Burst strength [kg/cm ²]
AEM	125	1.7	95	1.8	6.5	2.8
CEM	135	2.0	99	1.5	6.5	2.8

^a Measured in 2 M NaCl solution.

 $25~\text{m}^3/\text{day}$, TDS in the permeate <0.5 g/L, and water recovery up to ~70%.

FilmTecTM SW30–4040 elements with 7.4 m² of active area each (polyamide thin-film composite membrane, DuPont Water Solutions) were selected. The main test conditions and the relevant results indicated by the manufacturer in the datasheet are: 32,000 ppm NaCl feed, applied pressure of 55 bar, $7.4 \, \text{m}^3$ /day permeate flowrate with 8% water

recovery. One pressure vessel with six RO elements was selected and constructed for the pilot plant. An acid dosing system was implemented for the RO modules due to the possible presence of carbonate species and a high pH (close to 8) in the feedwaters.

After chemical dosage, a high-pressure pump (180B3046 APP 2.5, Danfoss) fed the RO pressure vessel.

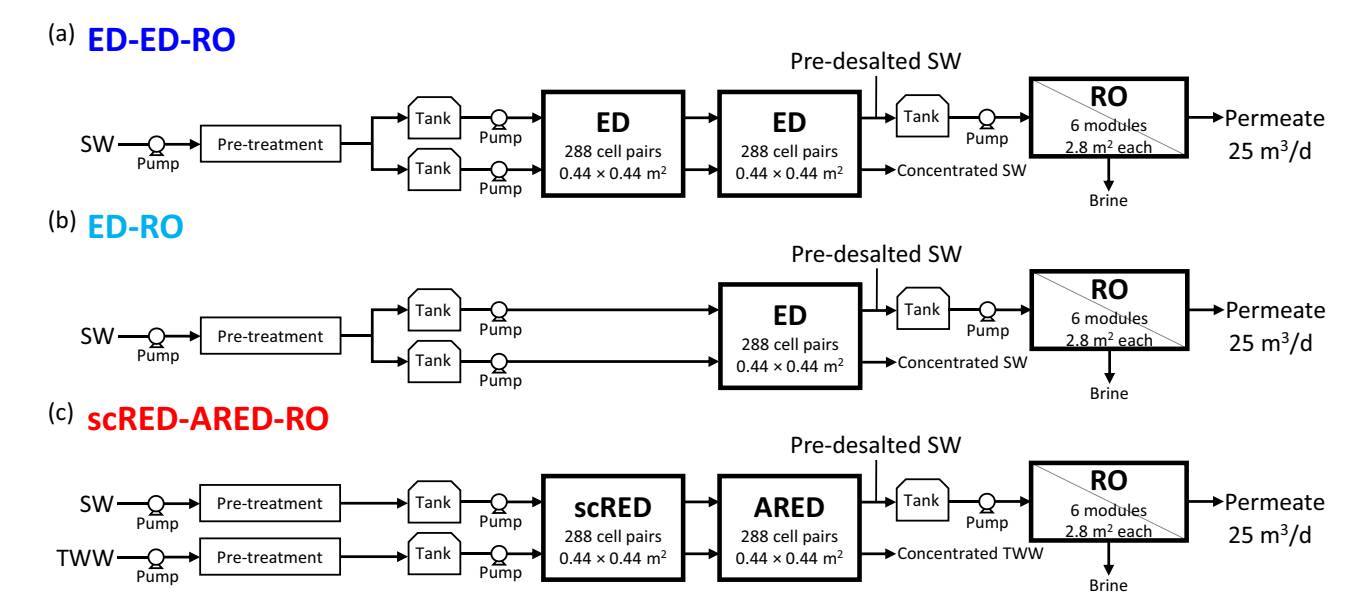


Fig. 4. Schematic diagrams of the tested pilot plant configurations: (a) ED-ED-RO, (b) ED-RO, and (c) scRED-ARED-RO.

 $^{^{\}rm b}$ Evaluated from measurements of membrane potential with 0.05 M and 0.5 M KCl solutions.

2.4. Experimental plan

The tested configurations of the pilot plant were ED-ED-RO, ED-RO, and scRED-ARED-RO, as schematically illustrated in Fig. 4. The double-stage of ED was adopted to boost the pre-desalination rate. An opposite strategy was adopted with the single-stage ED, which has a halved IEM area (and thus higher productivity) and can achieve a lower pre-desalination rate, due to the limiting current. The scRED-ARED configuration is somehow an intermediate case, because it had the same membrane area as the ED-ED configuration, but it was characterized by a lower total current value, which was similar to that of the single-stage ED (Section 3.1).

All field tests were conducted with the simple one-pass operation. Either one-stage or two-stage EM pre-desalination operation was tested. In the ED-RO tests, pre-treated seawater was fed into both the diluate and concentrate compartments of the first ED stack. In the ARED-RO tests, pre-treated seawater and wastewater were fed into the concentrate and diluate compartments, respectively, of the first stack. In the cases of two-stage EM pre-desalination, the second stack was fed by the outlet solutions coming from the first one.

The pre-desalted seawater produced by the EM processes (either ED or ARED) was collected in a buffer tank and pumped into the RO pressure vessel

Several tests were performed by letting the set points of the EM predesalination vary, as reported in Table 4. The test cases 1–7, 8, and 9–10 are for the ED-ED-RO, ED-RO (single stage ED before RO), and scRED-ARED-RO configuration, respectively. The outlet flow rates from the two compartments were chosen to have a water recovery in the EM predesalination around 63%. The pressure applied in the RO stage was adjusted to produce a nominal flow rate of permeate of 25 m³/day ($\pm 30\%$), corresponding to a total water recovery around 40%. The EM pre-desalination rate ranged from 35% to 51%. Clearly, RO completed the desalination process producing drinking water.

The EM processes were conducted with asymmetric flow rates. In particular, the flow rate of the pre-desalinated SW was higher than the flow rate of the pre-concentrated solution (SW or TWW), aiming at increasing the water recovery. However, to avoid excessive transmembrane pressures that could cause solution leakage, the flow rate of the pre-desalinated SW was no more than about twice the flow rate of the pre-concentrated solution. Higher flow rates in both compartments were used to reduce the relative detrimental effects of osmosis and/or electro-osmosis.

The typical duration of each test was between 90 and 120 min. Longrun tests were conducted for a duration up to height hours, showing a good stability of the plant. The accumulated operating time was of \sim 80 h, with experiments performed intermittently (due to restrictions related to the COVID 19 pandemic) during a period of about one year. However,

the performed experiments represent a meaningful set of tests, and the collected data provide interesting results and insights.

Errors in the measurements due to the parameters of the instruments (i.e., accuracy and resolution) were in the order of 0.1%. The error propagated in the calculation of the energy consumption remains in the same order of magnitude. Tests replicated under the same conditions showed a good reproducibility of the results (discrepancy in the order of 1%). For these reasons, error bars would be too small in the charts of the results, thus we did not report them.

2.5. Figures of merit characterizing the pilot plant performance

The feedwater ratio in the electromembrane pre-desalination process was defined as:

$$FR_{EM} = \frac{Q_{pre-des,in,EM}}{Q_{pre-des,in,EM} + Q_{pre-conc,in,EM}} \tag{1}$$

where $Q_{pre-des,in,EM}$ and $Q_{pre-conc,in,EM}$ are the volume flow rates of the pre-desalted (seawater) and pre-concentrated (seawater or TWW) solution, respectively, at the inlet of the EM stage. Water recovery of the EM process, of the RO, and total water recovery were calculated as:

$$WR_{EM} = \frac{Q_{pre-des,out,EM}}{Q_{pre-des,in,EM} + Q_{pre-conc,in,EM}}$$
 (2)

$$WR_{RO} = \frac{Q_{perm,RO}}{Q_{feed,RO}} \tag{3}$$

$$WR_{tot} = \frac{Q_{perm,RO}}{Q_{pre-des.in.EM} + Q_{pre-conc.in.EM}}$$
(4)

where $Q_{pre-des,out,EM}$ is the volume flow rate of the pre-desalted seawater at the outlet of the EM process, $Q_{perm,RO}$ and $Q_{feed,RO}$ are the volume flow rates of RO permeate and feed, respectively. The pre-desalted seawater from the EM stage was collected in a tank and then pumped to the RO pressure vessel. When the flow rate of pre-desalted seawater coincides with that of RO feed, the total water recovery is simply given by $WR_{tot} = WR_{EM} \cdot WR_{RO}$.

The specific production of desalted water per membrane area, called "productivity", was calculated for the EM processes and the RO as:

$$Prod_{EM} = \frac{Q_{pre-des,out,EM}}{A_{IEM}} \tag{5}$$

$$Prod_{RO} = \frac{Q_{perm,RO}}{A_{osm}} \tag{6}$$

where $A_{I\!E\!M}$ and A_{osm} are the total areas of ion-exchange membranes in

Table 4
Set points adopted in the electromembrane pre-desalination stage(s). "N.A." means "not applicable" and indicates either quantities not fixed as set points but obtained as results (i.e., the voltage drop in stage 1 for the ED-ED-RO tests and the pre-desalinated SW outlet conductivity from stage 1 for the scRED-RED-RO tests) or non-pertinent quantities (i.e., parameters regarding stage 1 for the ED-RO tests). The feedwater temperature recorded in the tests is also reported.

Configuration	Test case	Pre-desalinated SW outlet flow rate [L/ h]	Pre-concentrated solution (SW or TWW) outlet flow rate [L/h]	Pre-desalinated SW outlet conductivity from stage 1 [mS/cm]	Voltage drop in stage 1 [V]	Pre-desalinated SW outlet conductivity from stage 2 or single stage [mS/cm]	Feedwater temperature [°C]
ED-ED-RO	1	1555	766	36	N.A.	26	24.1
	2	1700	892	40	N.A.	26	22.4
	3	1500	1092	40	N.A.	26	21.9
	4	1500	820	40	N.A.	25	21.9
	5	1500	820	40	N.A.	30	19.4
	6	1500	820	40	N.A.	26	15.8
	7	1800	900	40	N.A.	26	15.3
ED-RO	8	1555	766	N.A.	N.A.	32.6	26.8
scRED-ARED- RO	9	2380	1140	N.A.	0	33.4	27.2 (SW), 26.6 (TWW)
	10	2380	1140	N.A.	0	33	27.9 (SW), 26.6 (TWW)

the EM stack(s) (either one or two) and in the RO modules. Clearly, the productivity of the RO process is the permeate flux.

The specific energy consumption of the EM process, of the RO, and the total specific energy consumption (excluding contributions of pretreatment and auxiliary components) were calculated as:

$$SEC_{EM} = \frac{\sum_{i} \Delta V_{i} \cdot I_{i}}{Q_{pre-des.out.EM}}$$
(7)

$$SEC_{RO} = \frac{Q_{feed,RO} \cdot p_{feed,RO} / \eta_{pump,RO}}{Q_{perm,RO}}$$
(8)

$$SEC_{tot} = \frac{\sum_{i} \Delta V_{i} \cdot I_{i} + Q_{feed,RO} \cdot p_{feed,RO} / \eta_{pump,RO}}{Q_{perm,RO}}$$
(9)

where ΔV_i and I_i are the voltage drop and the electric current supplied to the i-th stack (i.e., stack 1 or 2, with zero values for one stack in the case of single-stage ED), $p_{feed,RO}$ is the pressure applied to the RO feed upstream the pressure vessel, and $\eta_{pump,RO}$ is the efficiency of the pump pressurizing the RO feed (assumed equal to 0.9 [58]). Note that the SEC of each desalination stage (either EM or RO) has been defined per unit volume of its product water. Therefore, $SEC_{tot} \neq SEC_{EM} + SEC_{RO}$. In Eqs. (7) and (9) the DC drive efficiency and the pumping power consumption of the EM stage(s) are omitted, as they were negligible. Indeed, the former quantity was higher than 95% [59], and the latter, evaluated from the measured values of pressure drop in the EM stage(s), was below 0.1 kWh/m³.

The energy consumption of the pilot plant was also evaluated by considering the use of an energy recovery device (ERD). In this case, the *SEC* of the RO process can be estimated as:

$$SEC_{RO,ERD} = \frac{p_{feed,RO}}{\eta_{pump,RO}} \left[1 + \frac{1 - WR_{RO}}{WR_{RO}} (1 - \eta_{ERD}) \right]$$
 (10)

where η_{ERD} is the efficiency of the ERD (assumed equal to 0.9). Eq. (10) is obtained under the assumptions of equal flow rates sent through the ERD (pressure exchanger), negligible pressure drops in the pressure vessel, null pressure of the feed upstream the device and of the brine downstream the device, no mixing of the fluids, and equal efficiencies for the high- and low-pressure pumps. For the EM-RO integrated processes, the total energy consumption becomes:

$$SEC_{tot,ERD} = \frac{\sum_{i} \Delta V_{i} \cdot I_{i}}{Q_{perm,RO}} + \frac{p_{feed,RO}}{\eta_{pump,RO}} \left[1 + \frac{1 - WR_{RO}}{WR_{RO}} (1 - \eta_{ERD}) \right]$$
(11)

2.6. Baseline case: standalone SWRO

A baseline case of standalone SWRO was considered as benchmark for the integrated pilot plant performance. The baseline case was simulated by the RO model presented in a previous work [38]. The 6-module RO system (Section 2.3) was simulated with the following fixed conditions: feed concentration of 38.57 g/L (Table 1), feed temperature equal to the average value of the experimental test cases (22.2 °C), permeate flow rate of 25 m³/day, and water recovery equal to the average value of the WR_{tot} obtained with the integrated system (39.1%). The model predicted the pressure to be applied to the feed, the permeate concentration and the retentate concentration. The SEC was

evaluated with Eqs. (8) and (10) for the case without the ERD and with the ERD, respectively.

In the previous work [38], the RO model had been validated with ROSA and WAVE modelling tools by DuPont, finding a very good agreement. Now the RO model has been validated against the experimental data collected with the pilot plant. As shown in Table 5, the model predicted the permeate flux with values of discrepancy with the experimental data of few percent. Larger discrepancies were observed for the permeate conductivity. Overall, the agreement can be considered satisfactory, and the model can be considered reliable.

Note that the complete model [38] for EM-RO integrated processes was validated with data from the pilot testing, but this is beyond the scope of the present study.

3. Results and discussion

Results of the field-tests performed with the integrated pilot plant under different experimental conditions are summarized and discussed in the following. First, the electrical parameters of the electromembrane pre-desalination are presented. Then, the pressure applied in the RO stage and the permeate (product) conductivity are shown. Finally, the performance of the pilot plant is assessed by the main figures of merit.

3.1. Electromembrane pre-desalination: electrical parameters

The stack voltage and the current density applied in the EM predesalination to get the fixed setpoints (Table 4) are shown in Fig. 5. In the two-stage ED experiments (test cases 1–7), the voltage drop was between \sim 46 and 110 V (Fig. 5a). Note that the test cases 1–5 were characterized by high values of voltage drop in the first stage (\sim 97–110 V), while it was significantly lower in the test cases 6–7 (\sim 46–52 V). In the first tests, stack 1 exhibited some malfunctions that caused a high apparent resistance. However, they were then resolved by a successful stack revamping (see Appendix). The voltage drop in the second stage of the ED experiments was lower than \sim 65 V, and stack 2 did not suffer from high resistance as much as stack 1 before the revamping operation.

In the single-stage ED experiment (test case 8), the voltage drop was \sim 45 V, which was close to the minimum value of \sim 37–38 V characterizing stack 2 (ARED stage) for the scRED-ARED experiments (test cases 9 and 10). Of course, these test cases had zero voltage in the scRED stage (stack 1).

The current density ranged between \sim 145 and 212 A/m² in all test cases, apart from the scRED stage of the scRED-ARED experiments (test cases 9 and 10), where it was just below 60 A/m², as shown in Fig. 5b.

From these results, it can be drawn that the power consumption in the EM pre-desalination (see Eq. (9)) was in the descending order ED-ED > ED > scRED-ARED. Even when the values of voltage and current of the different test cases were comparable, the ED-ED configuration involved a higher power due to the sum of two contributions, while the ED and scRED-ARED configurations had only one stack consuming energy. Both voltage and current were higher in the single-stage ED configuration (test case 8) than in the scRED-ARED configuration (test cases 9 and 10). Moreover, the difference in the specific energy consumption between these two configurations will be accentuated by the higher flow rate of the pre-desalinated SW in the scRED-ARED cases (Table 4). Detailed data on the energy consumption will be reported and discussed in Section 3.3.

Table 5Comparison between RO model predictions and experimental data from the pilot plant.

	Test case 1		Test case 3			Test case 4			
	Experimental	Model	Discrepancy	Experimental	Model	Discrepancy	Experimental	Model	Discrepancy
Permeate conductivity [µS/cm]	378.33	484.04	28%	309.46	368.08	19%	664.12	419.33	-37%
Permeate flux [L/(m ² h)]	25.93	26.94	4%	30.78	31.22	1%	21.15	22.26	5%

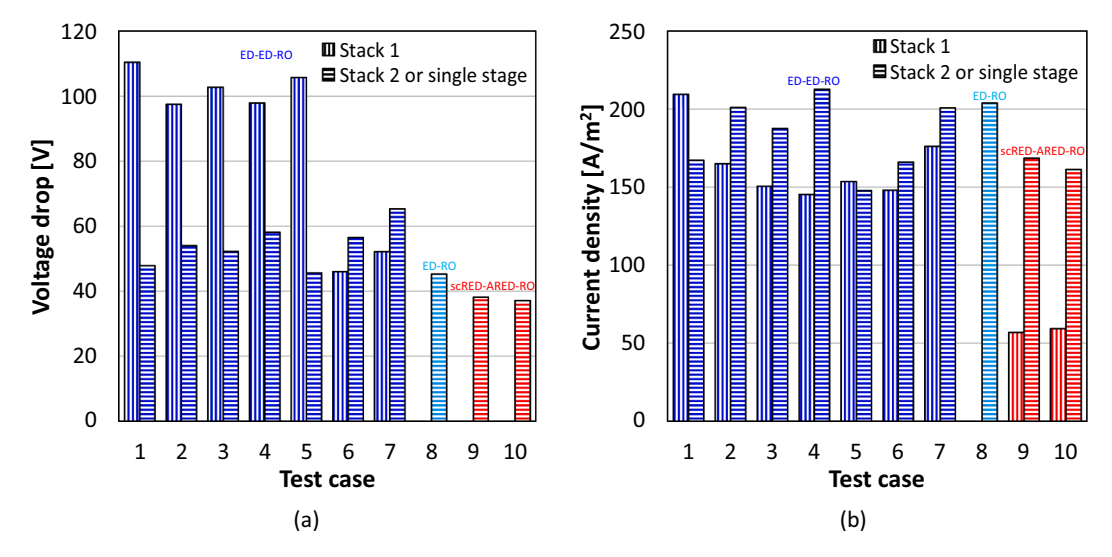


Fig. 5. Voltage drop (a) and current density (b) in the electromembrane pre-desalination processes needed to yield the setpoints reported in Table 4. Note that the test case 8 is with single-stage ED before RO, and the test cases 9 and 10 are with scRED, hence with zero voltage drop, in the first stack. The test cases 6–10 were performed after stacks revamping.

3.2. RO: applied pressure and product conductivity

Overall, the pressure applied to the RO feed (pre-desalinated seawater from the EM process) ranged from ~ 31 to 46 bar (Fig. 6a). The permeate conductivity was lower than $\sim 800~\mu\text{S/cm}$ in all the experiments, and equal to 540 $\mu\text{S/cm}$ on average (Fig. 6b), which means that drinking water quality for human use was achieved. The baseline case of the standalone SWRO required the highest pressure (~ 58 bar, Fig. 6a) and yielded the highest permeate conductivity, equal to $\sim 1068~\mu\text{S/cm}$ (Fig. 6b). For an NaCl solution at 20 °C, this value of electrical conductivity corresponds to a concentration of 525 mg/L [60], which is closer to the TDS limit of 600 mg/L recommended by WHO guidelines [61].

The RO feed pressurization level also affected the water flux and thus the product flow rate, as will be discussed in Section 3.3.

3.3. Performance of the pilot plant

Feedwater ratio and water recoveries are reported in Fig. 7. On average, the feedwater ratio was 72%, which is larger than the water recovery of the EM stage, i.e., $\sim 63\%$ on average. This difference can be

explained by the occurrence of a net water transport resulting from osmosis and electro-osmosis. In the ED tests, both mechanisms take place towards the same direction, i.e., from the pre-desalinated solution to the pre-concentrated solution, causing a reduction of the flow rate of the pre-desalinated seawater. In the test case 8, the halved IEM area reduced the difference between FR_{EM} and WR_{EM} . In the scRED and ARED conditions, electro-osmosis is towards the opposite direction with respect to osmosis. However, the values of WR_{EM} lower than those of FR_{EM} in the test cases 9 and 10 indicate that the electro-osmotic flux prevailed on the osmotic flux. The water recovery in the RO stage was between 31% and 63%, with values higher than 50–60% in most test

The total water recovery of the pilot plant with the hybrid EM-RO processes ranged from 27% to 51%. Note that WR_{tot} was not necessarily equal to the product of WR_{EM} times WR_{RO} , as the feed flow rate in the RO stage was not always identical to the outlet flow rate from the pre-desalination stage. It is worth noting that in the present scRED-ARED-RO configurations (test cases 9 and 10) the total water recovery calculated with respect to seawater feed only (i.e., excluding the impaired water) would be \sim 40%. Overall, the average water recovery of the hybrid pilot plant is 39.1%, corresponding to the value imposed in

10

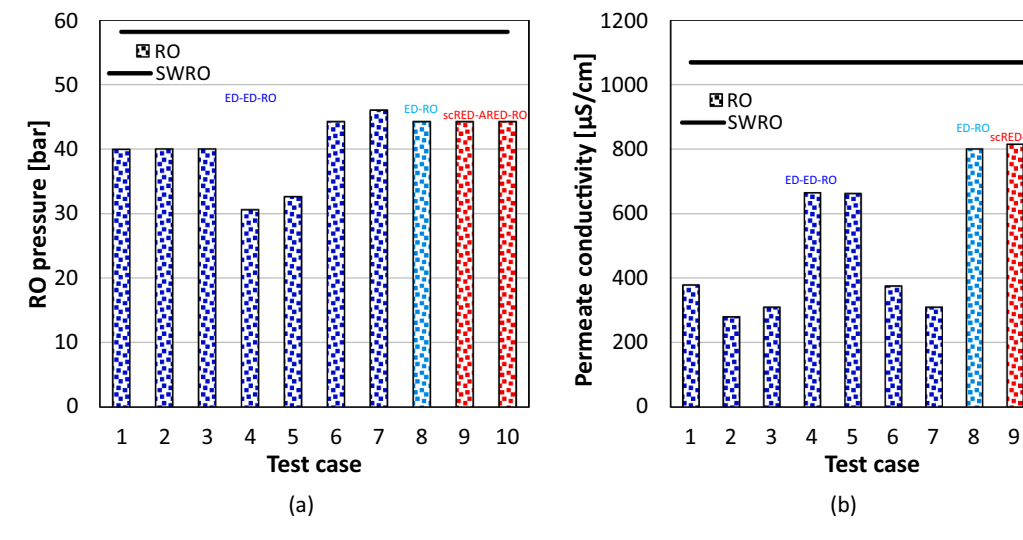


Fig. 6. Pressure applied to the RO feed (a) and electrical conductivity of the RO permeate (b). The baseline case of the standalone SWRO is also reported.

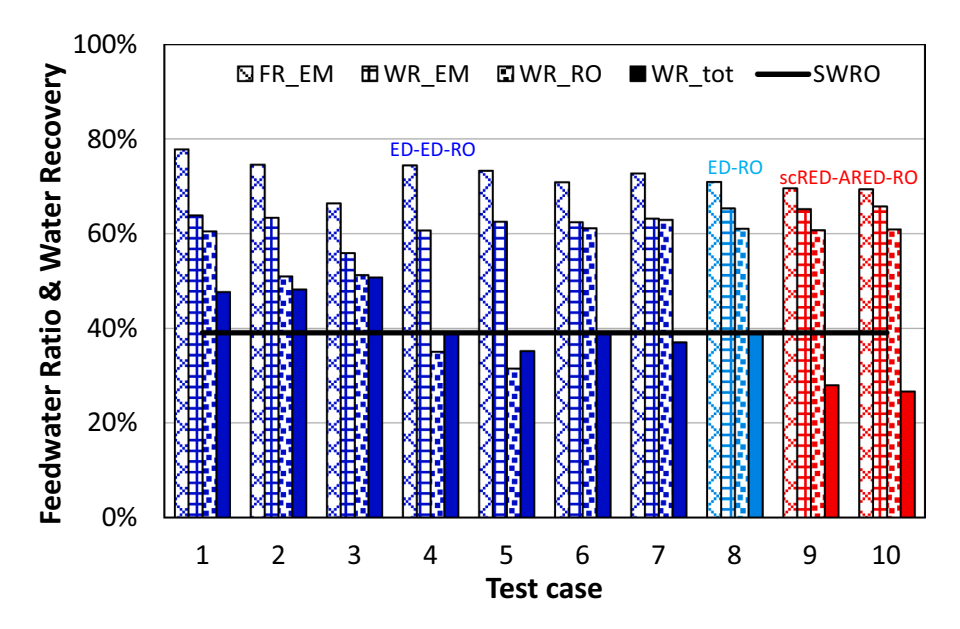


Fig. 7. Feedwater ratio in the electromembrane pre-desalination (FR_{EM}) needed to yield the setpoints reported in Table 4, and water recovery achieved in the EM pre-desalination (WR_{EM}), in the RO stage (WR_{RO}) and in the combined EM-RO process (WR_{tot}). The baseline case of the standalone SWRO is also reported.

the SWRO baseline case.

The values of productivity achieved by the pilot plant are reported in Fig. 8. In the two-stage ED experiments, the productivity was $\sim 7~L/(m^2~h)$, but this value was doubled in the single-stage ED (test case 8). Higher flow rates of seawater were used in the scRED-ARED experiments (see Table 4), so that the test cases 9 and 10 had a productivity of $\sim 10~L/(m^2~h)$. The productivity of the RO stage ranged from $\sim 19~to~31~L/(m^2~h)$, with an average value of $23.4~L/(m^2~h)$, which was set for the standalone SWRO baseline case. The obtained permeate flow rate, which can be simply calculated by multiplying the RO productivity times the RO membrane area (44.6 m²), was from 20.4 to 33.0 m³/day.

The values of specific energy consumption of the pilot plant are reported in Fig. 9 for two scenarios: system without any ERD, and system provided with an ERD. Looking at the former case, the ED-ED-RO configuration (test cases 1–7) had higher total energy consumptions ($\sim\!5.6{-}8.4\,\mathrm{kWh/m^3}$). It was caused by a high energy-consuming EM pre-

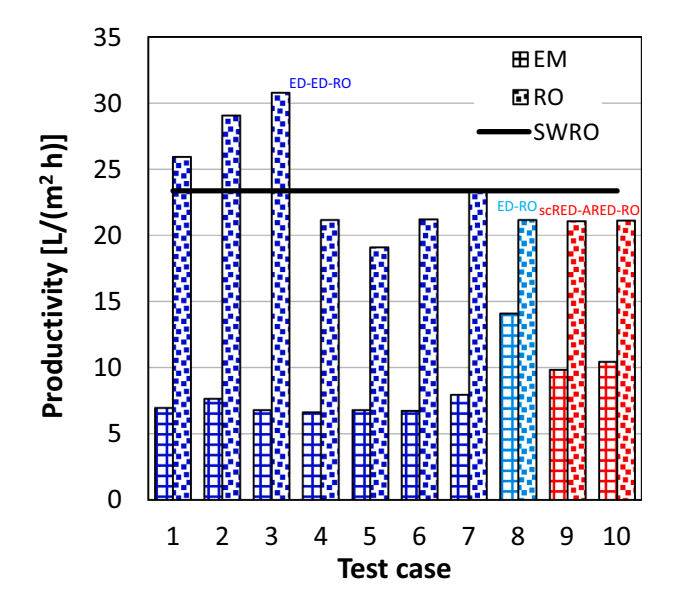


Fig. 8. Productivity of the EM pre-desalination and of the RO stage. The baseline case of the standalone SWRO is also reported.

desalination, not only before stacks revamping (test cases 1-5, with SEC_{EM} of $\sim 2.9-3.9$ kWh/m³), but also after that (test cases 6 and 7, with SEC_{EM} of ~2.1 and 2.4 kWh/m³, respectively). The ED-RO configuration (test case 8), instead, showed an energy consumption in the ED stage reduced to ~1.1 kWh/m³ and simultaneously maintained a low energy consumption, i.e., ~2.2 kWh/m³, in the RO stage, yielding an SEC_{tot} of ~ 4.1 kWh/m³. The scRED-ARED-RO configuration (test cases 9 and 10) further reduced the values of SEC_{EM} (~0.54 kWh/m³ on average), maintained the SEC_{RO} at ~ 2.3 kWh/m³, and attained the minimum SEC_{tot} of ~3.5 kWh/m³. With respect to the test case 9, the test case 10 was conducted with a small reduction in the setpoint of the conductivity of the pre-desalinated seawater (Table 4). However, due to some variations in the feedwater conductivity (salinity and temperature) the test case 10 attained a slightly lower SEC_{EM} and thus a lower SECtot. Under the operating conditions of the test cases 8, 9, and 10 without any ERD, the pilot plant exhibits values of SEC_{tot} (Eq. (9)) lower than the SEC of the standalone SWRO baseline (SEC_{SWRO}, Eq. (8)), which was 4.6 kWh/m³. Despite the additional contribution to the SEC_{tot} due to the EM processes, the EM-RO integrated system can be operated under conditions reducing the energy consumption compared to a standalone SWRO system.

In the scenario with the ERD, the energy consumption of the RO stage of the pilot plant ($SEC_{RO,ERD}$, Eq. (10)) and the total energy consumption ($SEC_{tot,ERD}$, Eq. (11)) were reduced on average by 42% and 18%, respectively, compared to the values obtained without the ERD (SEC_{RO} and SEC_{tot} , respectively). Instead, the energy consumption of the standalone SWRO configuration (SECSWRO,ERD, Eq. (10)) decreased by 55%, reaching 2.1 kWh/m³, which is 23% smaller than the lowest SEC_{tot}, ERD of the integrated system (test case 10). This occurs despite the SWRO system requires the highest pressure (Fig. 6). Indeed, a comparison between Eq. (10) and Eq. (11) shows that the standalone SWRO configuration saves the energy consumption of the EM stage. Moreover, there is an effect of the water recovery. The SWRO baseline case was performed by imposing a water recovery equal to the average value of the total water recovery of the integrated system, which implies that it is higher than the average water recovery of the RO stage of the integrated system. Therefore, the higher pressure required by the SWRO configuration is counter-balanced by these effects, leading to a lower energy consumption.

However, the ED-RO (test case 8) and scRED-ARED-RO (test cases 9 and 10) configurations exhibit values of $SEC_{tot,ERD}$ comparable to the

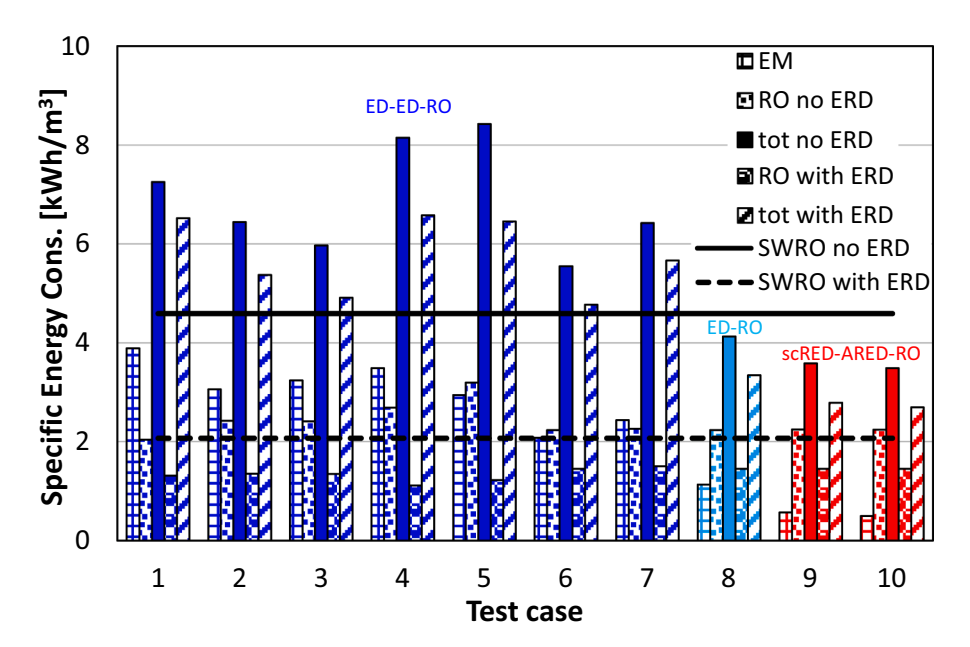


Fig. 9. Specific energy consumption of the EM pre-desalination, of the RO stage, and of the combined process. Two scenarios are considered for the RO (and thus for the total SEC): without ERD and with ERD. The baseline case of the standalone SWRO is also reported.

SEC_{SWRO,ERD}. The integrated system produced also a permeate with better quality (Fig. 6). Another simulation of the standalone SWRO process was performed by fixing the permeate conductivity at the mean value obtained with the integrated system, showing that the feed pressure would exceed the maximum value indicated by the manufacturer of the RO module.

4. Conclusions

A hybrid desalination plant at pilot scale combining electromembrane (EM) processes with reverse osmosis (RO) was demonstrated and tested for the first time for the production of drinking water from real seawater. The nominal capacity of the plant was $25~\text{m}^3$ /day. Electrodialysis (ED), shortcut reverse electrodialysis (scRED) and assisted reverse electrodialysis (ARED) were tested in the ED-ED-RO, ED-RO, and scRED-ARED-RO configurations. In the scRED-ARED-RO test cases, treated wastewater was used as impaired water acting as salt sink.

Pre-treatments, periodic polarity reversal, and chemical dosage were effective in the prevention of fouling and scaling. However, cost-effective strategies should be assessed in future studies.

The total water recovery of the integrated plant was around 40%. The productivity of the EM processes was $\sim 7\, L/(m^2\,h)$ in the ED-ED test cases and $\sim 10\, L/(m^2\,h)$ in the scRED-ARED test cases. The maximum value of $\sim 14\, L/(m^2\,h)$ was achieved by using a single stack (single-stage ED test). The RO stage produced a permeate with a flux of $\sim 20{-}30\, L/(m^2\,h)$. The lower productivity of the EM treatment may represent an issue due to the high cost of ion-exchange membranes. The use of a lower membrane area may be a possible strategy to reduce the capital cost.

The specific energy consumption was $\sim 5.6-8.4~\text{kWh/m}^3$ in the ED-ED-RO tests, while it reduced at $\sim 4.1~\text{kWh/m}^3$ with the ED-RO configuration. Therefore, a lower area of ion-exchange membranes can be beneficial for also reducing the operating cost. The scRED-ARED system further reduced the energy consumption of the pre-desalination, reaching the minimum value of total energy consumption of $\sim 3.5~\text{kWh/m}^3$. Therefore, the (A)RED process represents an interesting alternative for applications with co-located seawater desalination plants and WWTPs.

Overall, the specific energy consumption of the integrated pilot plant was comparable with that of a standalone SWRO system. In the absence

of any ERD, ED-RO and scRED-ARED-RO tests with the pilot plant outperformed the standalone SWRO system (4.6 kWh/m³). By considering the use of an efficient ERD, the energy consumption was lower for the SWRO (\sim 20% smaller than the minimum value of the integrated plant). However, the integrated system was able to produce drinking water with better quality (average conductivity of 540 $\mu S/cm$, against \sim 1000 $\mu S/cm$ of the SWRO system).

Customized modules should be developed to enhance the process performance. For example, RO modules suitable for treating "diluted SW" may have a higher water permeability. Further studies should address the techno-economic optimization of EM-RO integrated systems of industrial size by considering both design and operating conditions. In this perspective, the availability of validated modelling tools is crucial for the development of cost-effective systems to be proposed to the desalination market.

Nomenclature

 A_{IEM}

	electromembrane process [m ²]
A_{osm}	total area of osmotic membrane used in the RO process [m ²]
FR_{EM}	feedwater ratio in the electromembrane process
I_i	electric current supplied to the <i>i</i> -th stack [A]
$Prod_{EM}$	productivity of the electromembrane process [L/(m ² h)]
$Prod_{RO}$	productivity of the RO process [L/(m ² h)]
$p_{feed,RO}$	pressure applied to the RO feed [Pa]
$Q_{feed,RO}$	flow rate of the RO feed [m ³ /s]
$Q_{perm,RO}$	flow rate of the RO permeate [m ³ /s]
Q _{pre-conc,i}	_{n,EM} flow rate of the pre-concentrated solution (seawater or
	treated wastewater) at the inlet of the electromembrane
	process [m ³ /s]

total area of ion-exchange membranes used in the

 $Q_{pre-des,in,EM}$ flow rate of the pre-desalted seawater at the inlet of the electromembrane process [m³/s]

 $Q_{pre-des,out,EM}$ flow rate of the pre-desalted seawater at the outlet of the electromembrane process [m³/s]

 SEC_{EM} specific energy consumption of the electromembrane process $\lceil kWh/m^3 \rceil$

SEC_{RO} specific energy consumption of the RO process [kWh/m³] SEC_{RO,ERD} specific energy consumption of the RO process with the energy recovery device [kWh/m³]

 SEC_{SWRO} specific energy consumption of the SWRO process [kWh/m³] $SEC_{SWRO,ERD}$ specific energy consumption of the SWRO process with

the energy recovery device [kWh/m³]

 SEC_{tot} total specific energy consumption of the integrated process

[kWh/m³]

 $SEC_{tot,ERD}$ total specific energy consumption of the integrated process

with the energy recovery device [kWh/m³]

WR_{EM} water recovery of the electromembrane process

 WR_{RO} water recovery of the RO process

 WR_{tot} total water recovery of the integrated process

Greek symbols

 ΔV_i voltage drop at the *i*-th stack [V]

 $\eta_{pump,RO}$ efficiency of the pump for the pressurization of the RO feed

 η_{ERD} efficiency of the energy recovery device

CRediT authorship contribution statement

Luigi Gurreri: Software, Validation, Formal analysis, Data curation, Writing – original draft, Writing – review & editing, Visualization, Supervision. **Mariagiorgia La Cerva:** Software, Validation, Formal analysis, Investigation, Writing – original draft, Visualization. **Jordi Moreno:** Conceptualization, Methodology, Investigation, Resources,

Writing – original draft, Project administration, Funding acquisition. **Berry Goossens:** Conceptualization, Methodology, Resources, Writing – original draft, Project administration, Funding acquisition. **Andrea Trunz:** Conceptualization, Methodology, Resources, Writing – original draft, Project administration, Funding acquisition. **Alessandro Tamburini:** Conceptualization, Methodology, Resources, Writing – original draft, Supervision, Project administration, Funding acquisition.

Declaration of competing interest

The authors declare that they have no known competing financial interests or personal relationships that could have appeared to influence the work reported in this paper.

Acknowledgments

This work was performed in the framework of the REvivED water project (Low energy solutions for drinking water production by a REvival of ElectroDialysis systems). This project has received funding from the European Union's Horizon 2020 Research and Innovation program under Grant Agreement no. 685579 (www.revivedwater.eu).

The authors are grateful to Deukum GmbH for supplying the spacers, and to FACSA for providing their facilities for the plant installation.

Appendix: Overhaul and refurbishment of stacks

During the first testing period (test cases 1–5 in the main text), stack 1 exhibited a high electrical resistance (see Section 3.1). Therefore, both stacks were inspected to check their conditions from the inside. After removing the distribution side-plates, the first observation was a large amount of white deposition at the inlets/outlets of the channels close to the electrode chambers of stack 1 (Fig. A1). The analysis of deposition samples detected both Ca and Mg salts, most likely CaCO₃ and Mg(OH)₂.

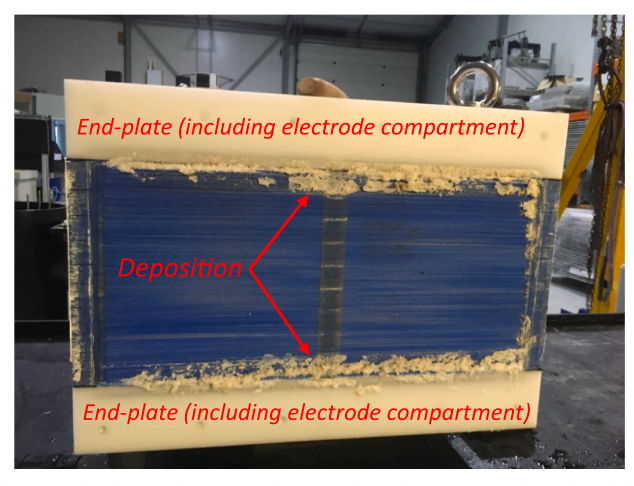


Fig. A1. Stack 1 after taking away the distribution side-plates. The picture shows a white deposition at the outlet of the channels near the electrode compartments (~5–10 cell pairs).

The stack overhaul detected (i) a severe damage (a hole) in the end-membranes, (ii) a loss of their transport properties, and (iii) a severe internal leakage. Other membranes showed minor shift in performance. It is not clear what caused the failure of stack 1, but probably it is related with a leakage of ERS. It certainly occurred through the damaged end-membranes, but some initial leakage from the gaskets (not perfect sealing) cannot be excluded. The triggered precipitation/deposition near the electrode compartments caused a partial blockage of channels in those parts of the stack. This led to a local over-depletion of ions in the desalting compartments and thus to a higher stack resistance. On the other hand, it caused a lower limiting current density. Water splitting occurring at high voltage favoured the precipitation of salts by a pH increase. This all might have caused the burned/damaged membranes.

A stack revamping was then performed by replacing the damaged membranes. For stack 2, which did not show problems, only the end-membranes were replaced. The new end-membranes (two layers) used for both stacks were chlorine- and pH-resistant Fumatech membranes (Fumasep® F-10100), as the ERS used in the tests after stack refurbishment was maintained at a pH of 3.5 and chlorine could be formed due to NaCl diffusion. After revamping, the resistance of stack 1 was reduced by ~50% and the tests did not show the issues that characterized the initial experiments.

Finally, it is worth mentioning that no fouling was observed on the membrane surface during the stack overhaul, thus indicating that the pre-treatment was successful. In the experiments, the conductivity of the concentrated seawater from the first stage was between \sim 68 and 82 mS/cm, while that from the second stage was between \sim 85 and 97 mS/cm. However, no scaling was observed, likely due to the acid dosage against carbonate

precipitation and to the spacer effectiveness against concentration polarization.

References

- E. Jones, M. Qadir, M.T.H. van Vliet, V. Smakhtin, S. Kang, The state of desalination and brine production: a global outlook, Sci. Total Environ. 657 (2019) 1343–1356, https://doi.org/10.1016/j.scitotenv.2018.12.076.
- [2] J. Eke, A. Yusuf, A. Giwa, A. Sodiq, The global status of desalination: an assessment of current desalination technologies, plants and capacity, Desalination 495 (2020), 114633, https://doi.org/10.1016/j.desal.2020.114633.
- [3] L.F. Greenlee, D.F. Lawler, B.D. Freeman, B. Marrot, P. Moulin, Reverse osmosis desalination: water sources, technology, and today's challenges, Water Res. 43 (2009) 2317–2348, https://doi.org/10.1016/j.watres.2009.03.010.
- [4] M. Elimelech, W.A. Phillip, The future of seawater desalination: energy, technology, and the environment, Science 333 (2011) 712–717, https://doi.org/ 10.1126/science.1200488, 80-.
- [5] H. Nassrullah, S.F. Anis, R. Hashaikeh, N. Hilal, Energy for desalination: a state-of-the-art review, Desalination 491 (2020), 114569, https://doi.org/10.1016/j.desal.2020.114569
- [6] V.G. Gude, Desalination and sustainability an appraisal and current perspective, Water Res. 89 (2016) 87–106, https://doi.org/10.1016/j.watres.2015.11.012.
- [7] G. Amy, N. Ghaffour, Z. Li, L. Francis, R.V. Linares, T. Missimer, S. Lattemann, Membrane-based seawater desalination: present and future prospects, Desalination 401 (2017) 16–21, https://doi.org/10.1016/j.desal.2016.10.002.
- [8] N. Voutchkov, Energy use for membrane seawater desalination current status and trends, Desalination 431 (2018) 2–14, https://doi.org/10.1016/j. desal 2017 10 033
- [9] J. Kim, K. Park, D.R. Yang, S. Hong, A comprehensive review of energy consumption of seawater reverse osmosis desalination plants, Appl. Energy 254 (2019), 113652, https://doi.org/10.1016/j.apenergy.2019.113652.
- [10] C. Skuse, A. Gallego-Schmid, A. Azapagic, P. Gorgojo, Can emerging membranebased desalination technologies replace reverse osmosis? Desalination 500 (2021), 114844 https://doi.org/10.1016/j.desal.2020.114844.
- [11] A. Campione, L. Gurreri, M. Ciofalo, G. Micale, A. Tamburini, A. Cipollina, Electrodialysis for water desalination: a critical assessment of recent developments on process fundamentals, models and applications, Desalination 434 (2018) 121–160, https://doi.org/10.1016/j.desal.2017.12.044.
- [12] F.E. Ahmed, A. Khalil, N. Hilal, Emerging desalination technologies: current status, challenges and future trends, Desalination 517 (2021), 115183, https://doi.org/ 10.1016/j.desal.2021.115183.
- [13] S.K. Patel, P.M. Biesheuvel, M. Elimelech, Energy Consumption of Brackish Water Desalination: Identifying the Sweet Spots for Electrodialysis and Reverse Osmosis, ACS ES&T Eng, 2021, https://doi.org/10.1021/acsestengg.0c00192 acsestengg.0c00192.
- [14] A. Daniilidis, R. Herber, D.A. Vermaas, Upscale potential and financial feasibility of a reverse electrodialysis power plant, Appl. Energy 119 (2014) 257–265, https://doi.org/10.1016/j.apenergy.2013.12.066.
- [15] R.A. Tufa, S. Pawlowski, J. Veerman, K. Bouzek, E. Fontananova, G. di Profio, S. Velizarov, J. Goulão Crespo, K. Nijmeijer, E. Curcio, Progress and prospects in reverse electrodialysis for salinity gradient energy conversion and storage, Appl. Energy 225 (2018) 290–331, https://doi.org/10.1016/j.apenergy.2018.04.111.
- [16] R.W. Baker, Membrane Technology and Applications, John Wiley & Sons, Ltd, Chichester, UK, 2012, https://doi.org/10.1002/9781118359686.
- [17] M.M. Generous, N.A.A. Qasem, U.A. Akbar, S.M. Zubair, Techno-economic assessment of electrodialysis and reverse osmosis desalination plants, Sep. Purif. Technol. 272 (2021), 118875, https://doi.org/10.1016/j.seppur.2021.118875.
- [18] L. Bazinet, T.R. Geoffroy, Electrodialytic processes: market overview, membrane phenomena, recent developments and sustainable strategies, Membranes (Basel). 10 (2020) 221, https://doi.org/10.3390/membranes10090221.
- [19] L. Gurreri, A. Tamburini, A. Cipollina, G. Micale, Electrodialysis applications in wastewater treatment for environmental protection and resources recovery: a systematic review on progress and perspectives, Membranes (Basel). 10 (2020) 146, https://doi.org/10.3390/membranes10070146.
- [20] A. Campione, A. Cipollina, I.D.L. Bogle, L. Gurreri, A. Tamburini, M. Tedesco, G. Micale, A hierarchical model for novel schemes of electrodialysis desalination, Desalination 465 (2019) 79–93, https://doi.org/10.1016/J.DESAL.2019.04.020.
- [21] M. La Cerva, L. Gurreri, M. Tedesco, A. Cipollina, M. Ciofalo, A. Tamburini, G. Micale, Determination of limiting current density and current efficiency in electrodialysis units, Desalination 445 (2018) 138–148, https://doi.org/10.1016/j. desal 2018 07 028
- [22] L. Gurreri, A. Filingeri, M. Ciofalo, A. Cipollina, M. Tedesco, A. Tamburini, G. Micale, Electrodialysis with asymmetrically profiled membranes: Influence of profiles geometry on desalination performance and limiting current phenomena, Desalination 506 (2021), 115001, https://doi.org/10.1016/j.desal.2021.115001.
- [23] G. Battaglia, L. Gurreri, M. Ciofalo, A. Cipollina, I.D.L. Bogle, A. Pirrotta, G. Micale, A 2-D model of electrodialysis stacks including the effects of membrane deformation, Desalination 500 (2021), 114835, https://doi.org/10.1016/j. desal.2020.114835
- [24] G. Doornbusch, M. van der Wal, M. Tedesco, J. Post, K. Nijmeijer, Z. Borneman, Multistage electrodialysis for desalination of natural seawater, Desalination 505 (2021), 114973, https://doi.org/10.1016/j.desal.2021.114973.

- [25] G.J. Doornbusch, M. Tedesco, J.W. Post, Z. Borneman, K. Nijmeijer, Experimental investigation of multistage electrodialysis for seawater desalination, Desalination 464 (2019) 105–114, https://doi.org/10.1016/J.DESAL.2019.04.025.
- [26] G. Doornbusch, H. Swart, M. Tedesco, J. Post, Z. Borneman, K. Nijmeijer, Current utilization in electrodialysis: electrode segmentation as alternative for multistaging, Desalination 480 (2020), 114243, https://doi.org/10.1016/j. desal.2019.114243.
- [27] G.J. Doornbusch, M. Bel, M. Tedesco, J.W. Post, Z. Borneman, K. Nijmeijer, Effect of membrane area and membrane properties in multistage electrodialysis on seawater desalination performance, J. Memb. Sci. 611 (2020), 118303, https://doi. org/10.1016/j.memsci.2020.118303.
- [28] J. Jang, Y. Kang, J.H. Han, K. Jang, C.M. Kim, I.S. Kim, Developments and future prospects of reverse electrodialysis for salinity gradient power generation: Influence of ion exchange membranes and electrodes, Desalination 491 (2020), 114540, https://doi.org/10.1016/j.desal.2020.114540.
- [29] S. Pawlowski, R.M. Huertas, C.F. Galinha, J.G. Crespo, S. Velizarov, On operation of reverse electrodialysis (RED) and membrane capacitive deionisation (MCDI) with natural saline streams: A critical review, Desalination 476 (2020), 114183, https://doi.org/10.1016/J.DESAL.2019.114183.
- [30] H. Tian, Y. Wang, Y. Pei, J.C. Crittenden, Unique applications and improvements of reverse electrodialysis: a review and outlook, Appl. Energy 262 (2020), 114482, https://doi.org/10.1016/j.apenergy.2019.114482.
- [31] A. Zoungrana, M. Çakmakci, From non-renewable energy to renewable by harvesting salinity gradient power by reverse electrodialysis: a review, Int. J. Energy Res. 45 (2021) 3495–3522, https://doi.org/10.1002/er.6062.
- [32] A. Tamburini, A. Cipollina, M. Tedesco, L. Gurreri, M. Ciofalo, G. Micale, The REAPower project: power production from saline waters and concentrated brines, in: A. Basile, E. Curcio, I. Inamuddin (Eds.), Curr. Trends Futur. Dev. Membr. -Membr. Desalin. Syst. Next Gener, Elsevier, Amsterdam, 2019, pp. 407–448, https://doi.org/10.1016/B978-0-12-813551-8.00017-6.
- [33] J.Y. Nam, K.S. Hwang, H.C. Kim, H. Jeong, H. Kim, E. Jwa, S.C. Yang, J. Choi, C. S. Kim, J.H. Han, N. Jeong, Assessing the behavior of the feed-water constituents of a pilot-scale 1000-cell-pair reverse electrodialysis with seawater and municipal wastewater effluent, Water Res. 148 (2019) 261–271, https://doi.org/10.1016/j.watres.2018.10.054.
- [34] S. Mehdizadeh, Y. Kakihana, T. Abo, Q. Yuan, M. Higa, Power generation performance of a pilot-scale reverse electrodialysis using monovalent selective ionexchange membranes, Membranes (Basel) 11 (2021) 27, https://doi.org/10.3390/ membranes11010027.
- [35] A.M. Hulme, C.J. Davey, S. Tyrrel, M. Pidou, E.J. McAdam, Scale-up of reverse electrodialysis for energy generation from high concentration salinity gradients, J. Membr. Sci. 627 (2021), 119245, https://doi.org/10.1016/j. memsci.2021.119245.
- [36] R. Pärnamäe, L. Gurreri, J. Post, W.J. van Egmond, A. Culcasi, M. Saakes, J. Cen, E. Goosen, A. Tamburini, D.A. Vermaas, M. Tedesco, The acid-base flow battery: sustainable energy storage via reversible water dissociation with bipolar membranes, Membranes (Basel). 10 (2020) 409, https://doi.org/10.3390/ membranes10120409.
- [37] A. Culcasi, L. Gurreri, G. Micale, A. Tamburini, Bipolar membrane reverse electrodialysis for the sustainable recovery of energy from pH gradients of industrial wastewater: Performance prediction by a validated process model, J. Environ. Manag. 287 (2021), 112319, https://doi.org/10.1016/j. jenvman.2021.112319.
- [38] M. La Cerva, L. Gurreri, A. Cipollina, A. Tamburini, M. Ciofalo, G. Micale, Modelling and cost analysis of hybrid systems for seawater desalination: electromembrane pre-treatments for reverse osmosis, Desalination 467 (2019) 175–195, https://doi.org/10.1016/j.desal.2019.06.010.
- [39] F.E. Ahmed, R. Hashaikeh, N. Hilal, Hybrid technologies: the future of energy efficient desalination – a review, Desalination 495 (2020), 114659, https://doi. org/10.1016/j.desal.2020.114659.
- [40] M. Herrero-Gonzalez, R. Ibañez, Chemical and energy recovery alternatives in SWRO desalination through electro-membrane technologies, Appl. Sci. 11 (2021) 8100. https://doi.org/10.3390/app11178100.
- [41] R.K. McGovern, S.M. Zubair, J.H. Lienhard V., The cost effectiveness of electrodialysis for diverse salinity applications, Desalination 348 (2014) 57–65, https://doi.org/10.1016/j.desal.2014.06.010.
- [42] R.K. McGovern, A.M. Weiner, L. Sun, C.G. Chambers, S.M. Zubair, J.H. Lienhard V., On the cost of electrodialysis for the desalination of high salinity feeds, Appl. Energy 136 (2014) 649–661, https://doi.org/10.1016/j.apenergy.2014.09.050.
- [43] A.H. Galama, M. Saakes, H. Bruning, H.H.M. Rijnaarts, J.W. Post, Seawater predesalination with electrodialysis, Desalination 342 (2014) 61–69, https://doi. org/10.1016/j.desal.2013.07.012.
- [44] J.W. Post, H. Huiting, E.R. Cornelissen, H.V.M. Hamelers, Pre-desalination with electro-membranes for SWRO, Desalin. Water Treat. 31 (2011) 296–304, https://doi.org/10.5004/dwt.2011.2400.
- [45] T.N. Bitaw, K. Park, J. Kim, J.W. Chang, D.R. Yang, Low-recovery, -energy-consumption, -emission hybrid systems of seawater desalination: energy optimization and cost analysis, Desalination 468 (2019), 114085, https://doi.org/10.1016/j.desal.2019.114085.
- [46] S. Thampy, G.R. Desale, V.K. Shahi, B.S. Makwana, P.K. Ghosh, Development of hybrid electrodialysis-reverse osmosis domestic desalination unit for high recovery

- of product water, Desalination 282 (2011) 104–108, https://doi.org/10.1016/j.
- [47] J.M. Wreyford, J.E. Dykstra, K. Wetser, H. Bruning, H.H.M. Rijnaarts, Modelling framework for desalination treatment train comparison applied to brackish water sources, Desalination 494 (2020), 114632, https://doi.org/10.1016/j. desal.2020.114632.
- [48] B.M. Yang, J.M. Li, Z.Y. You, W.L. Lai, C.M. Kao, Using integrated electrodialysis and RO hybrid system to remediate and reclaim perchlorate-contaminated groundwater, Desalination 480 (2020), 114377, https://doi.org/10.1016/j. desal.2020.114377.
- [49] K. Loganathan, P. Chelme-Ayala, M. Gamal El-Din, Treatment of basal water using a hybrid electrodialysis reversal-reverse osmosis system combined with a lowtemperature crystallizer for near-zero liquid discharge, Desalination 363 (2015) 92–98, https://doi.org/10.1016/j.desal.2015.01.020.
- [50] X. Zhang, C. Zhang, F. Meng, C. Wang, P. Ren, Q. Zou, J. Luan, Near-zero liquid discharge of desulfurization wastewater by electrodialysis-reverse osmosis hybrid system, J. Water Process Eng. 40 (2021), 101962, https://doi.org/10.1016/j. iwne.2021.101962.
- [51] Y. Mei, C.Y. Tang, Co-locating reverse electrodialysis with reverse osmosis desalination: synergies and implications, J. Memb. Sci. 539 (2017) 305–312, https://doi.org/10.1016/j.memsci.2017.06.014.
- [52] L. Gurreri, G. Battaglia, A. Tamburini, A. Cipollina, G. Micale, M. Ciofalo, Multiphysical modelling of reverse electrodialysis, Desalination 423 (2017) 52–64, https://doi.org/10.1016/j.desal.2017.09.006.
- [53] M. Ciofalo, M. La Cerva, M. Di Liberto, L. Gurreri, A. Cipollina, G. Micale, Optimization of net power density in reverse electrodialysis, Energy 181 (2019) 576–588, https://doi.org/10.1016/j.energy.2019.05.183.

- [54] L. Gómez-Coma, V.M. Ortiz-Martínez, M. Fallanza, A. Ortiz, R. Ibañez, I. Ortiz, Blue energy for sustainable water reclamation in WWTPs, J. Water Process Eng. 33 (2020), 101020, https://doi.org/10.1016/j.jwpe.2019.101020.
- [55] W. Li, W.B. Krantz, E.R. Cornelissen, J.W. Post, A.R.D. Verliefde, C.Y. Tang, A novel hybrid process of reverse electrodialysis and reverse osmosis for low energy seawater desalination and brine management, Appl. Energy 104 (2013) 592–602, https://doi.org/10.1016/j.apenergy.2012.11.064.
- [56] M. Vanoppen, E. Criel, S. Andersen, A.R.D. Verliefde, Assisted reverse electrodialysis: a novel technique to decrease reverse osmosis energy demand, in: AMTA/AWWA Membr. Technol. Conf. Pap. 32, American Membrane Technology Association (AMTA); American Water Works Association (AWWA), 2016, pp. 1–12. https://biblio.ugent.be/publication/7098263.
- [57] M. Vanoppen, E. Criel, G. Walpot, D.A. Vermaas, A. Verliefde, Assisted reverse electrodialysis—principles, mechanisms, and potential, Npj Clean Water. 1 (2018) 9, https://doi.org/10.1038/s41545-018-0010-1.
- [58] Danfoss, The Heart of Seawater RO Systems: Rugged APP High-pressure Pumps. htt ps://assets.danfoss.com/documents/187154/AD243586503052en-001102.pdf. (Accessed 25 November 2021).
- [59] SM15K Series Products, Delta-Elektronika.nl, https://www.delta-elektronika.nl/en/products/bidirectional-dc-power-supplies-15kw-sm15k-series.html (Accessed 25 November 2021).
- [60] S.S. Islam, R.L. Gupta, K. Ismail, Extension of the Falkenhagen-Leist-Kelbg equation to the electrical conductance of concentrated aqueous electrolytes, J. Chem. Eng. Data 36 (1991) 102–104, https://doi.org/10.1021/je00001a031.
- [61] WHO, Guidelines for Drinking-water Quality, 2017.